Journal of Nuclear Materials 395 (2009) 45–49

Contents lists available at ScienceDirect

Journal of Nuclear Materials

journal homepage: www.elsevier.com/locate/jnucmat

Helium atoms in chromium-rich Fe–Cr alloys – *Ab initio* results

K.O.E. Henriksson

Department of Chemistry, University of Helsinki, P.O. Box 55, FIN-00014, Finland

ARTICLE INFO

Article history:
Received 10 August 2009
Accepted 27 September 2009

PACS:
71.20.Be
61.72.J–
31.15.A–

Keywords:
Helium
Chromium
Density-functional theory
Defects

ABSTRACT

Helium generation in Fe–Cr alloys degrades the material by causing swelling and eventually the nucleation of bubbles. When the alloys are used as construction materials the resulting embrittlement is especially undesirable. The effects of helium atoms in pure iron have been recently elucidated by *ab initio* calculations. The different magnetic behavior – ferromagnetic for iron and anti-ferromagnetic for chromium – makes simple extrapolation to alloys and pure chromium uncertain. In the present study helium in pure chromium as well as chromium alloys with a small concentration of iron is investigated by *ab initio* density-functional theory calculations. The results indicate that interstitial helium atoms occupy the tetrahedral site in pure chromium. A pair of interstitial helium atoms have binding energies of about 0.3–0.6 eV when they are first or second nearest neighbors. When a substitutional iron atom is involved, the binding energy goes up to 1 eV. The formation energy of a substitutional helium atom is slightly higher (about 0.2 eV) when a substitutional iron atom is close by. The same holds for two helium atoms sitting in a vacancy, but then the energy difference is roughly twice as large. A substitutional helium atom is relatively strongly bound to a substitutional iron atom, with a binding energy of about 0.3 eV.

1. Introduction

Stainless steels – essentially Fe–Cr alloys with some alloying elements – used in fission (and future fusion) reactor constructions suffer damage due to neutron irradiation. Beside the creation of point defects, the neutrons are also responsible for transmutation reactions, producing helium ions [1]. Due to its low solubility in metals, helium atoms are strongly trapped and tend to gather into bubbles (see Refs. [2,3] and references therein). These bubbles lead to decreased mobility of dislocations, resulting in swelling and embrittlement of the metal. The neutron flux will be higher in fusion reactors than in fission reactors, so the effects of helium generation are particularly detrimental in that case.

The effects of helium in pure iron have recently been investigated on the *ab initio* level [4–7]. The Fe–Cr alloys to be used in future fusion reactors will most likely contain about 10-wt% Cr [8], a level which has been proved to provide the strongest resistance to swelling. Limited data exist for helium in chromium.

The goal of the present study is to shed some light on the behavior of helium atoms in pure chromium, and chromium with trace amounts of iron in close proximity to the helium atoms. For this *ab initio* density-functional theory calculations are used. The results indicate that many of the considered defect systems are bound. Examples of bound systems include: (i) helium atoms in single vacancies, (ii) close by interstitial helium atoms, and (iii) interstitial helium atoms close to substitutional iron atoms. The common feature for these is that they consist of interstitial helium atoms. The insertion of helium into the chromium–iron systems need not be "damaging", e.g. creating vacancies that become filled with helium, in order for the defects to form.

2. Methods

The *ab initio* density-functional theory (DFT) calculations were carried out using the projector augmented wave (PAW) method [9] in a plane-wave basis set as implemented in the Vienna *ab* initio simulation package (VASP) [10–14]. Pseudopotentials employing the local density approximation with the Ceperley–Alder exchange correlation as parametrized by Perdew and Zunger [15], and extended with generalized gradient approximation (GGA) corrections developed by Perdew and Wang [16,17] were used. The calculations are therefore all at the GGA level. Also, to improve on the magnetic moments and magnetic energies, the interpolation formula by Vosko et al. [18] was used. These were taken from the database supplied with VASP.

The sampling of *k*-points in the Brillouin zone was done with the Monkhorst–Pack scheme [19]. The integration over the Brillouin zone was carried out with the Methfessel–Paxton (MP) method [20] and the linear tetrahedron (LT) method of Blöchl et al. [21]. The MP method was used in all structure relaxations, and the LT method was only used when accurate energies of relaxed structures were calculated.

E-mail address: krister.henriksson@helsinki.fi

0022-3115/$ - see front matter © 2009 Elsevier B.V. All rights reserved.
doi:10.1016/j.jnucmat.2009.09.014

Table 1
Lattice parameters and cohesive energies of ferromagnetic (FM) bcc Fe, antiferromagnetic (AFM) bcc Cr, and isolated helium atoms.

System	Lattice parameter (nm)	VASP cohesive energy (eV)
Fe (FM)	0.2830	−8.209
Cr (AFM)	0.2848	−9.470
He	–	0.0

All the present calculations are based on supercells with 128 metal lattice sites forming a body centered cubic (bcc) lattice. The cell is made up of four conventional cubic cells in each Cartesian direction, making it contain 64 unit cells. A total number of $3 \times 3 \times 3$ k-points were used, with an energy cutoff of 400 eV. Lower or equal cutoff energies have been used in studies [22,23,6,4] for the Fe–Cr, Fe–He, and Cr–He systems, with similar values for these settings. Full relaxation of both cell parameters (size and shape) and atomic coordinates was performed. The calculations were considered converged when the changes in the forces on individual atoms became less than 10^{-5} eV/nm^2. The residual pressure in the relaxed cells was always checked, and the calculations were continued if the pressure was over 1 kbar. All calculations were spin-polarized.

It should be noted that the true ground state for chromium at zero Kelvin is a spin density wave (SDW) (see Ref. [24]). Using the GGA, the ground state is antiferromagnetic (AFM) bcc Cr [24], with the SDW being higher in energy. However, with a nonlocal exchange correlation potential [25] it may be possible to generate non-collinear magnetic moments (including SDWs) that are lower in energy than the AFM state. Given the preliminary nature of these results, and their higher computational cost, the AFM state is used as the ground state in the present study. The ordering of energies for configurations with the same number of Cr atoms should not be affected, even if the SDW were to be considered the true ground state. Since mostly comparisons between different configurations involving the same number of impurities (He and Fe) are carried out in Section 3, the choice of AFM as the ground state should not have any large bearing on any qualitative findings.

The formation energy of a system containing n_i atoms of species S_i is in this study defined as

$$E_f(S_1,\ldots) = E(S_1,\ldots) - \sum_i n_i E(S_i), \tag{1}$$

where $E(S_1,\ldots) < 0$ is the potential energy of the (bulk) system, and $E(S_i)$ is the energy per atom of the individual elements in their reference states. These are taken as ferromagnetic (FM) bcc iron, AFM bcc chromium, and isolated helium atoms. The numerical values can be found in Table 1 in Section 3.1 below.

The binding energy of a defect system $A_1 + \cdots + A_n$ (such as substitutional Cr close to tetrahedral He), where A_i is a fundamental defect, is [26]

$$E_b(A_1 + \cdots + A_n) = \sum\nolimits_i E(A_i) - E(A_1 + \cdots + A_n) - (n-1)E_{\text{ref}}, \tag{2}$$

where $E(A_i)$ is the energy of the cell containing only defect A_i, $E(A_1 + \cdots + A_n)$ is the energy of the cell containing the defect system, and E_{ref} is the energy of the cell without any defects. If $E_b < 0$ then it is energetically favorable for the defects to be far apart, and the system can be said to be repulsive or unbound.

3. Results and discussion

3.1. Reference energies

The energies of the reference states used for calculation of formation energies are presented in Table 1.

Table 2
Formation energies E_f and binding energies E_b for simple defects in Cr involving He. The initial distance between the two interstitial He atoms in the last two cases is one lattice parameter. See Section 3.2 for an explanation of the abbreviations.

System	E_f (eV)	E_b (eV)
Vacancy	2.60	
Tetr. He	5.13	
Oct. He	5.30	
⟨1 1 1⟩ Cr–He	5.13[a]	
Subst. He (He_1V)	4.93	
He_2V	7.78	2.28
He_3V	11.09	4.10
He_4V	15.56	4.75
He_5V	17.58	7.86
He_6V	21.49	9.07
He_7V	24.59	11.10
He_8V	28.92	11.89
He_9V	33.23	12.71
Oct. He_2, 1NN and 2NN	9.64	0.61
Tetr. He_2, 1NN	10.00	0.25
Tetr. He_2, 2NN	9.72	0.53
Tetr. He_2, 4NN	10.26	−0.01

[a] Relaxes to tetrahedral site.

3.2. Helium in chromium

The formation and binding energies of simple He-related defects in Cr are shown in Table 2. The binding energies for defects involving only He atoms and no vacancies are with respect to isolated tetrahedral He atoms. The binding energies for defects involving N He atoms and one vacancy are with respect to one substitutional He atom and $N-1$ tetrahedral He atoms.

The relative ordering of the formation energies of substitutional, tetrahedral, and octahedral He in bcc Cr follows the same trend as for He in bcc Fe [4,5]. The significant difference is that the values in the Cr case are all roughly 1 eV higher, meaning He insertion into Cr costs more energy than into Fe. In both metals an interstitial He atom prefers the tetrahedral site. From the table, the tetrahedral site is 0.17 eV lower in energy than the octahedral site. Corresponding value for He in Fe is about 0.2 eV [4,5].

Concerning the relation between interstitial and substitutional energies for He in Cr, the data indicate that the octahedral (tetrahedral) site is 0.37 eV (0.20 eV) higher than the substitutional one. This is in agreement with a similar study of He in Cr by Domain [23], where the difference is 0.43 eV (0.23 eV). The present value for the vacancy formation is about 0.1 eV lower than in Ref. [22], where the volume was not allowed to relax during the calculations.

Single helium atoms are quite strongly trapped in mono-vacancies, with a binding energy of 2.79 eV. The corresponding value for iron is 2.30 eV [5], i.e. about 0.5 eV lower. In other words, He atoms in Cr-vacancies are more strongly bound than in Fe-vacancies. The binding energy rises monotonically when the helium content of a monovacancy is increased. The largest content tried was nine He atoms. The relaxed atomic positions for nine He atoms in a monovacancy is shown in Fig. 1.

The relaxed configurations of helium atoms in a monovacancy are as follows: (i) the atoms in He_2V assume a ⟨1 1 1⟩ orientation. The interatomic distance is 0.153 nm. (ii) The He atoms in He_3V form a isosceles triangle, with side lengths 0.171 nm and 0.160 nm (the base). The normal of the triangle is in the ⟨1 0 0⟩ direction. (iii) A perfect square with a ⟨1 0 0⟩ normal is formed by the He in He_4V, with all sides of length 0.163 nm. (iv) The He atoms in He_5V form a pyramid, with a basal square with side length 0.170 nm, and the top He atom at a distance of 0.176 nm from all the other He atoms. (v) A perfect octahedron is formed by the He atoms in He_6V, the distance between He neighbors being 0.175 nm. The octahedron consists of two pyramids with their square basal planes joined together. (vi) When a He atom is placed

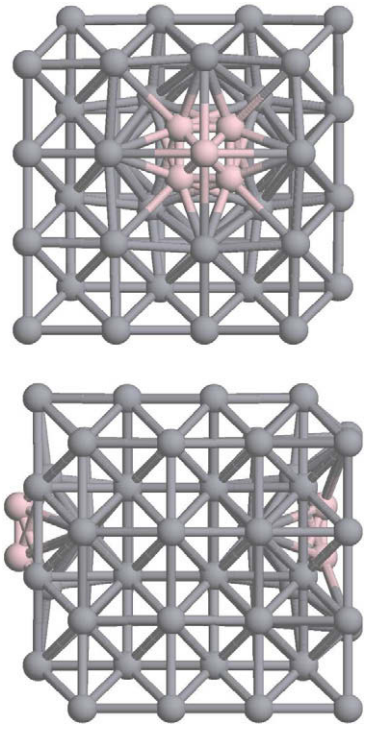

Fig. 1. (Color online.) Relaxed configuration with nine He atoms (light pink) inside a vacancy in AFM bcc Cr. (For interpretation of the references to colour in this figure legend, the reader is referred to the web version of this article.)

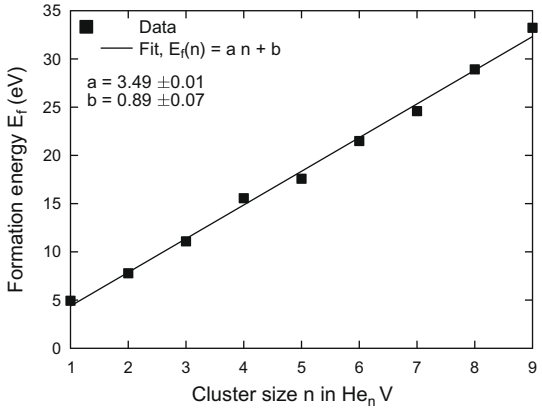

Fig. 2. Cluster formation energy as a function of cluster size n in He_nV. A linear fit is also shown.

at the center of the octahedron to form the He_7V cluster, the side lengths change. The side length of the square basal plane increases to 0.206 nm. The He atoms at the top of the pyramids are 0.205 nm from the He atoms in the square. The He atom placed in the center of the former octahedron is at a distance of 0.145 nm from the nearest neighbor. (vii) The He atoms in He_8 forms a perfect cube, with side length 0.152 nm. The side planes of the cube have normals $\langle 1\,0\,0\rangle$. (viii) One can obtain He_9V by adding one He to the center of this cube. The resulting parallelepiped has side lengths of 0.165 nm and 0.166 nm. The centered He atom is at a distance of 0.143 nm and 0.144 nm from the atoms forming the He "cage".

A plot of the formation energy as a function of cluster size n is shown in Fig. 2 together with a linear fit $E_f(n) = an + b$. The value of the fitted parameters are $a = 3.49 \pm 0.01$ eV and $b = 0.89 \pm 0.07$ eV. The uncertainties in the parameters stem from synthetic errors set to $0.10|E_f|$ for each data point (n, E_f).

There is another way to define the binding energies of He_NV clusters, than using a substitutional He atom and $N-1$ tetrahedral atoms. Perhaps a more natural choice is to use a tetrahedral He atom and a vacancy containing $N-1$ He atoms as the fundamental defects. The binding energy is then simply the energy required to break off one He atom from the cluster. This energy may be called "cluster binding energy" and denoted E_N. Its definition is:

$$E_N \equiv E_b(\mathrm{He_T} + \mathrm{He}_{N-1}\mathrm{V}) = E(\mathrm{He_T}) + E(\mathrm{He}_{N-1}\mathrm{V}) - E_{\mathrm{ref}} - E(\mathrm{He}_N\mathrm{V}), \quad (3)$$

where $E(\mathrm{He_T})$ is the energy of the cell containing a tetrahedral He atom, $E(\mathrm{He}_N\mathrm{V})$ is the energy of a cell containing N He atoms in a vacancy, and E_{ref} is the energy of a cell without any defects. The cluster binding energies are plotted in Fig. 3. From the figure it can be seen that the clusters He_5V and He_7V are particularly strongly bound with respect to emission of a He atom into a tetrahedral position far away from the cluster.

The general trend of the present results for small values of N agree with those for He in Fe, which show an initially decreasing trend, with binding energies between 2 and 3 eV [5,7]. A similar oscillatory behavior is also observed by Seletskaia et al. [27] in a molecular dynamics study of multiple He in a Fe monovacancy.

Not only the vacancy-related defects show a binding nature. Also some of the purely interstitial defects mentioned on the last four lines in Table 2 constitute strongly bound complexes. Two octahedral helium atoms, initially placed either as first (1NN) or second (2NN) nearest neighbors, end up in the same configuration, namely as a $\langle 2\,1\,0\rangle$ He–He interstitial. The He–He interatomic distance is 0.155 nm, a little more than half the lattice parameter $a = 0.2835$ nm of perfect AFM bcc Cr at zero Kelvin. The 1NN and 2NN distances correspond to $a/2$ and $\sqrt{2}a/2$, respectively.

For two helium atoms on tetrahedral sites there are no similar geometric changes. In these cases the He atoms have not moved much after relaxation. Two tetrahedral He atoms placed at a distance corresponding to fourth nearest neighbors (4NN), are not bound to each other at all. In this case the 1NN, 2NN, and 4NN distances correspond to $\sqrt{2}a/4$, $a/2$, and a, respectively. For a pair of tetrahedral He atoms placed as 2NN, the binding energy is relatively high, 0.53 eV, as shown in Table 2. The corresponding result for He in Fe is 0.3 eV [6], i.e. almost a factor two smaller.

The surprising result by Seletskaia et al. [4] that helium atoms in iron acquire a magnetic moment carries only partly over to the case of helium in chromium. For He in Fe, magnetic moment values of $0.015\mu_B$, $0.012\mu_B$, and $0.000\mu_B$ were obtained for (relaxed) octahedral, tetrahedral, and substitutional He, respectively [4]. Here μ_B is the Bohr magneton. The present calculations for

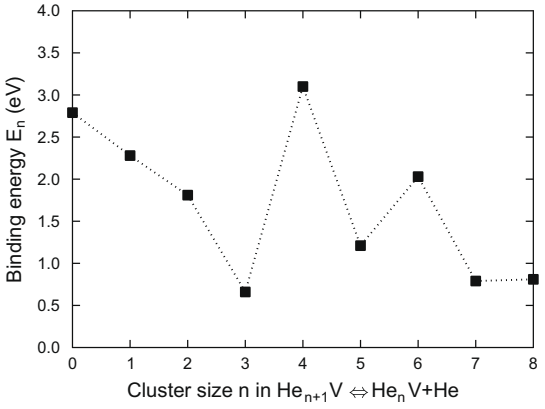

Fig. 3. Cluster binding energies E_N as a function of the cluster size N. The broken line is a guide for the eye.

Table 3
As in Table 2, but with Fe as a foreign species. See Section 3.2 for an explanation of the abbreviations.

System	E_f (eV)	E_b (eV)
Subst. Fe (Fe_1V)	0.48	
Subst. Fe_2 (Fe_2V_2), 1NN	0.81	0.14
Subst. Fe_2 (Fe_2V_2), 2NN	0.99	−0.04
Subst. Fe_2 (Fe_2V_2), ∞	0.95	0.00

Table 4
Formation energies E_f and binding energies E_b for simple defects in Cr involving He and Fe. See Fig. 4 for the initial configurations of the defects. See Section 3.2 for an explanation of the abbreviations.

	System	E_f (eV)	E_b (eV)
(a)	⟨1 1 1⟩ Fe–He	5.86	−0.26
	Fe–oct. He, 1NN	5.45	0.15
	Fe–tetr. He, 1NN	5.43	0.17
	Fe–oct. He, 2NN	5.56	0.04
	Fe–tetr. He, 2NN	5.52	0.08
(b)	Fe—He_1V, 1NN	5.11	0.30
	Fe—He_1V, 2NN	5.17	0.24
(c)	Fe—He_2V, 1NN	8.21	2.33, 0.04[a]
(d)	Fe–oct. He_2 (He–He: 2NN)	9.73	1.00
(e)	Fe–tetr. He_2 (He–He: 2NN) (ground state)	9.73	1.00
(f)	Fe–tetr. He_2 (He–He: 4NN)	9.73	1.00
(g)	Fe_2 (1NN)–oct. He	5.71	0.36
(h)	Fe_2 (1NN)–tetr. He	5.74	0.34
(i)	Fe_2 (2NN)–oct. He	5.75	0.32
(j)	Fe_2 (2NN)–tetr. He	5.82	0.26

[a] With respect to a He_2V cluster.

antiferromagnetic Cr give $0.007\mu_B$, $0.000\mu_B$, and $0.01\mu_B$, for the same cases. In other words, the present values are one order of magnitude smaller than for He in Fe, except for the substitutional helium atom, where it is of the same order as for interstitial He in Fe. The four first nearest neighbors of the substitutional He atom (in Cr) have $1.051\mu_B$, and the six second nearest neighbors have $-0.936\mu_B$. In comparison, in pure antiferromagnetic Cr the average magnitude of the magnetic moment is $0.874\mu_B$. Olsson et al. [22] report a lower value of $0.92\mu_B$, which might however be due to the lower cutoff energy of 300 eV. These results indicate that He behaves as a paramagnetic ion in both iron and chromium, with the magnetic moment pointing in the same direction as the closest metallic neighbors.

3.3. Iron in chromium

The formation and binding energies of Fe-related defects in Cr are shown in Table 3. These are used when calculating the binding energies of Fe–He defects. The binding energy of the Fe pair is with respect to two non-interacting substitutional Fe atoms.

As a side note, these results indicate that substitutional Fe atoms placed close to each other form a complex that is stable even at room temperature, assuming that the contribution from entropy stays small (room temperature corresponds to a kinetic energy of about 0.026 eV, according to the equipartition theorem). Increasing their mutual initial distance to one lattice parameter changes the attraction into a repulsion. At infinite separation the binding energy of the Fe atom pair is naturally zero (last row of Table 3).

3.4. Helium in chromium–iron alloys

The formation and binding energies of He- and Fe-related defects in Cr are shown in Table 4. Some of the defects are illustrated in Fig. 4.

The binding energies are always with respect to substitutional Fe atoms, infinitely separated if there is more than one of these. Binding energies for defects containing single He atoms and no vacancies are with respect to tetrahedral He atoms. If a vacancy is involved, then the binding energies are with respect to one substitutional He atom and $N-1$ tetrahedral atoms, where N is the total number of He atoms in the defect system.

From the table it is seen that the defect system consisting of a substitutional Fe, a Cr, and an interstitial He, all sitting on a line in the ⟨1 1 1⟩ direction, is unbound. If the Fe atom would be replaced by a Cr atom, the He atom would relax to the closest tetrahedral site (see Table 2). On the other hand, if the He atom were to be brought closer to the Fe atom – into a tetrahedral or octahedral site – the defect system would again be bound, with binding energies $\leqslant 0.17$ eV, as can be seen in Table 4.

Single substitutional Fe atoms bind single interstitial He atoms, with energies varying between 0.04 eV and 0.17 eV. Upon introduction of a monovacancy the binding energies grow larger. A substitutional He is bound to a substitutional Fe with an energy

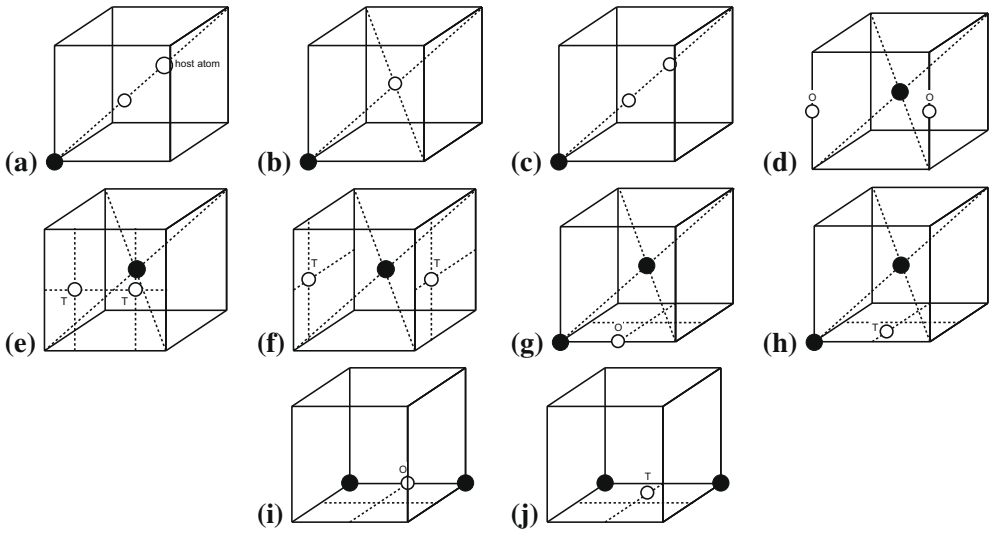

Fig. 4. Initial defect configurations for He (open thin circles) and substitutional metal impurities (black filled circles) in a metal host. See Table 4 for formation and binding energies. 'T' means tetrahedral site, and 'O' octahedral site.

of 0.24—0.30 eV. If a single substitutional Fe atom is accompanied by two interstitial He atoms the binding energy is 1.00 eV, with a quite high formation energy of 9.73 eV. In all of the three investigated cases the final relaxed state is the same, namely case (e) in Table 4. Introducing an extra substitutional Fe atom and removing one of the two interstitial He atoms the binding energy goes down to 0.26—0.36 eV.

4. Conclusions

Ab initio density-functional theory calculations of He defects in antiferromagnetic Cr show that many of the considered defects form bound systems. According to the results individual interstitial He atoms occupy the tetrahedral site in pure antiferromagnetic bcc Cr. A pair of interstitial He atoms form a bound system with binding energies of about 0.3—0.6 eV when they are first or second nearest neighbors. When they are close to a substitutional Fe atom the binding energy goes up to 1 eV. The formation energy of a substitutional He atom is somewhat higher (about 0.2 eV) when a substitutional Fe atom is close by. The same holds for two He atoms sitting in a vacancy, but then the energy difference is roughly twice as large. A substitutional He atom is relatively strongly bound to a substitutional Fe atom, with a binding energy of about 0.3 eV. These results indicate that He atoms inserted into Cr with Fe impurities will form bound defect systems even if the insertion is not accompanied with the creation of vacancies.

Acknowledgments

A part of the electronic structure calculations presented in this article have been carried out in the CSC's computing environment. CSC is the Finnish IT center for science and is owned by the Ministry of Education.

The author is thankful for useful discussions with Nils Sandberg (Department of Reactor Physics, Royal Institute of Technology, Stockholm) and computational resources provided by Prof. Kai Nordlund (Department of Physics, University of Helsinki). The author thanks Christophe Domain for providing software for the analysis of local magnetic moments from VASP output.

References

[1] R.E. Stoller, J. Nucl. Mater. 174 (1990) 289.
[2] H. Trinkaus, B. Singh, J. Nucl. Mater. 323 (2003) 229–242.
[3] K.O.E. Henriksson, K. Nordlund, J. Keinonen, Nucl. Instr. Meth. Phys. Res. B 244 (2006) 377–391.
[4] T. Seletskaia, Y. Osetsky, R.E. Stoller, G.M. Stocks, Phys. Rev. Lett. 94 (4) (2005) 046403.
[5] C.-C. Fu, F. Willaime, Phys. Rev. B 72 (2005) 064117.
[6] L. Ventelon, B. Wirth, C. Domain, J. Nucl. Mater. 351 (2006) 119–132.
[7] C.-C. Fu, F. Willaime, J. Nucl. Mater. 367–370 (2007) 244–250.
[8] E.E. Bloom, J.T. Busby, C.E. Duty, P.J. Maziasz, T.E. McGreevy, B.E. Nelson, B.A. Pint, P.F. Tortorelli, S.J. Zinkle, J. Nucl. Mater. 367–370 (2007) 1–10.
[9] P.E. Blöchl, Phys. Rev. B 50 (24) (1994) 17953–17979.
[10] G. Kresse, J. Hafner, Phys. Rev. B 47 (1) (1993) 558–561.
[11] G. Kresse, J. Hafner, Phys. Rev. B 49 (20) (1994) 14251–14269.
[12] G. Kresse, J. Furthmüller, Comp. Mater. Sci. 6 (1996) 15–50.
[13] G. Kresse, J. Furthmüller, Phys. Rev. B 54 (16) (1996) 11169–11186.
[14] G. Kresse, D. Joubert, Phys. Rev. B 59 (3) (1999) 1758–1775.
[15] J.P. Perdew, A. Zunger, Phys. Rev. B 23 (10) (1981) 5048–5079.
[16] J.P. Perdew, J.A. Chevary, S.H. Vosko, K.A. Jackson, M.R. Pederson, D.J. Singh, C. Fiolhais, Phys. Rev. B 46 (11) (1992) 6671–6687.
[17] Y. Wang, J.P. Perdew, Phys. Rev. B 44 (24) (1991) 13298–13307.
[18] S.H. Vosko, L. Wilk, M. Nusair, Can. J. Phys. 58 (1980) 1200.
[19] H.J. Monkhorst, J.D. Pack, Phys. Rev. B 13 (12) (1976) 5188–5192.
[20] M. Methfessel, A.T. Paxton, Phys. Rev. B 40 (6) (1989) 3616–3621.
[21] P.E. Blöchl, O. Jepsen, O.K. Andersen, Phys. Rev. B 49 (23) (1994) 16223–16233.
[22] P. Olsson, C. Domain, J. Wallenius, Phys. Rev. B 75 (1) (2007) 014110.
[23] C. Domain, J. Nucl. Mater. 351 (2006) 1–19.
[24] R. Hafner, D. Spisak, R. Lorenz, J. Hafner, Phys. Rev. B 65 (18) (2002) 184432.
[25] K. Capelle, L.N. Oliveira, Phys. Rev. B 61 (22) (2000) 15228–15240.
[26] C. Domain, C.S. Becquart, J. Foct, Phys. Rev. B 69 (2004) 144112.
[27] T. Seletskaia, Y.N. Osetsky, R.E. Stoller, G.M. Stocks, J. Nucl. Mater. 351 (2006) 109–118.